

# Theoretical Study For Bond Between Reinforcement Steel And Concrete

U. M. MAHRAN

*Associate Prof., Civil Eng. Dept., Assiut University, Assiut 71516, Egypt*

## Abstract

The behavior and load carrying behavior of reinforced concrete structures is influence by the interaction between the concrete and reinforcement. The stress transfer between reinforcement and concrete in the longitudinal direction of the bars is called bond. An essential feature of reinforced concrete is the bond between steel and concrete. Anchorage of reinforcement depends on the bond between steel and concrete, crack width and crack spacing are mainly governed by it. So, stiffness, deformation and dynamic behavior are influenced by it, and in reverse loading damping and energy dissipation is a function of bond. This is one of the reasons why bond has been, and still is, a topic of fundamental and applied research.

Bond stress is the equivalent unit shear stress acting in parallel to the reinforcing bar on the interface between reinforcing steel bar and concrete. Due to the transfer of forces through bond stress, between the reinforcing rebar and concrete, the force in the reinforcing bar changes along its length. Because bond stress is thought of as stress per unit area of bar surface, it is related to the rate of change of steel stress. Consequently, to have bond stress it is necessary to have a changing steel stress. In cases of high stress at the contact interface, near cracks or end anchorages, the bond stresses are related to relative displacements between concrete and steel. These relative displacements, which are caused by different average strains in the concrete and the steel, are usually called bond-slip ( $\tau$ - $\delta$ ).

**Keywords:** repairing; bond; ( $\tau$ - $\delta$ ), inteface, rib, crack

## 1-Introduction

Many variables have been investigated in regard to bond stress and deformation. However, due to the complex nature of the phenomenon and due to great difficulties in measuring the relevant properties in the vicinity of a steel bar in concrete there is still a lack of know-how and the general applicability of results is still insufficient. It was thought worthwhile to treat bond in a nonlinear numerical analysis by taking into account cracking and larger local deformations. If the method of material modeling and numerical procedure should be successful, it would be possible to treat numerous external and internal variables only by varying the material properties.

---

\* Usama MAHRAN. Tel: +20-1062489624; fax. +02-0862364636  
Email address: usamhrn1@yahoo.com

External variables could be loading rate, transverse stress, and temperature, whereas internal variables could be concrete composition, strength, bar surface, and dimensions. In all cases, the calculation would be the same, only the input parameters would be different.

Fig. 1 shows the relation that indicate clearly that, besides the bond-slip, a further variable X orientated along a beam's axis influences the local  $\tau$ -values considerably, references [1]., Fig 2 clearly shows that the bond stress developed by plain reinforcing bars is dependent on both the slip and the steel stress [2].

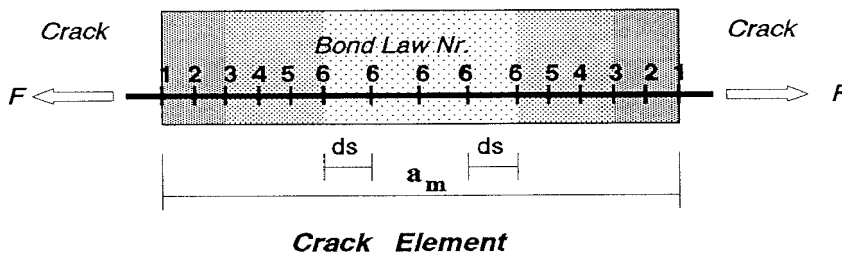
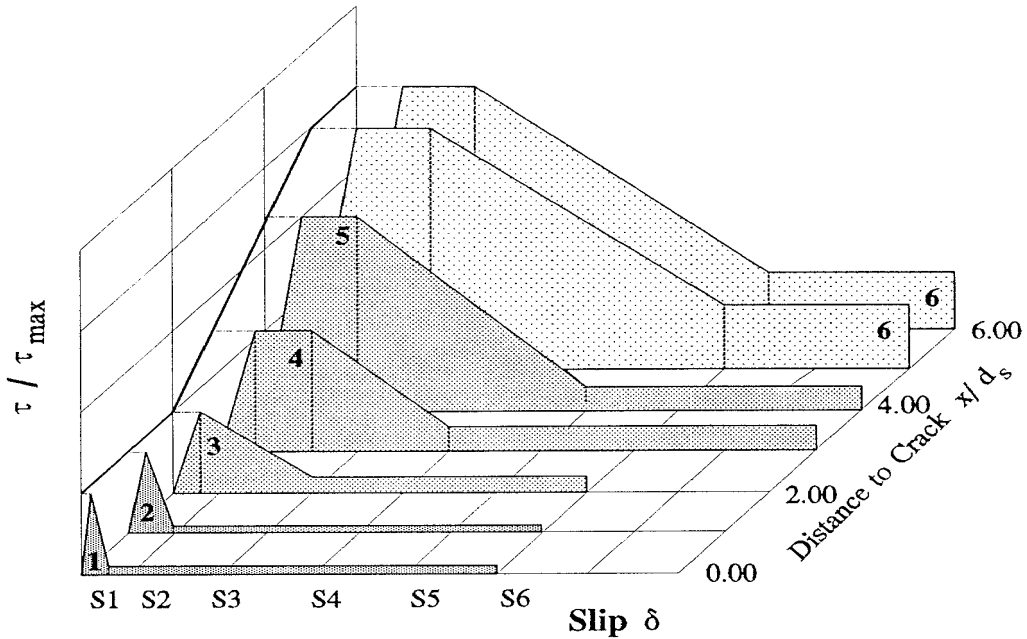


Fig. (1) Relation between the shear stresses, slips and distance to crack.

In fact, very little work has so far been done in this field. It is hypothesized that, in addition to bond stress and slip, confining pressure and steel strain are the main variables defining bond behavior. This is consistent with previous experimental results and is apparent in the following observations from experimental bond tests:

1-If confinement is not provided, bond stresses vanish as soon as the longitudinal crack develops through the cover.

2- The concrete cover itself provides confinement through tensile hoop stresses prior to cracking.

3- The ultimate resistance at large slips appears to be of the Coulomb friction type.

4- Bond stress is higher when bars are pushed instead of pulled (due to Poisson's effect).

5- The discrepancy in bond stress-slip relations appearing in the literature would be explained by the variations in the test specimens, which provide varying degrees of confinement.

6- Effects of concrete cover, bar position, end distance, and transverse reinforcement could be predicted via the confinement each provides.

These observations motivated the design of a new numerical modeling device that allows studying relevant parameters influencing the bond-slip behavior. Therefore, the main aim of this paper is to demonstrate that bond between deformed reinforcing bars and concrete can be predicted by numerical analysis taking account of non-linear effects. Therefore, an attempt has been made to model the bond behavior in a numerical way using the shape and properties of deformed reinforcing bars, and the properties of concrete.

## **2- Modeling description**

In this work, I try to simulate the bond between concrete and reinforcing steel bars using Interface Slide Line (ISL) elements as an element modeling of bond. This technique is not using the bond stress-slip relation as a material modeling. Although most analysis representations of bond tend to model the steel-to-concrete interface as a two-dimensional surface, the bond-transfer mechanism, including crushing and cracking, actually occurs in a finite zone surrounding the reinforcement (Gerstle and Ingraffea [3]). From an experimental point of view, this means that a process zone surrounding the reinforcement has to be defined, and the measured slip will actually include the deformations of this zone. In the present study, the process zone is arbitrarily assumed to be cylindrical with an outer diameter of 200 mm. The model consisted of a 22 mm diameter deformed bar embedded in a concrete cylinder 160 mm long. In attempt to obtain local characteristics, only five lugs were in contact with the concrete.

## **3- Material response characteristics of the elements**

### **3.1 Interface Slide Line element (ISL)**

In this study, we have used special interface elements for the connection of reinforcement steel elements to the concrete elements. These interface elements join steel elements and concrete elements together at the bar surface between lugs. In this analysis, two different values of friction coefficient are used ( $\mu = 0.30$  and  $\mu = 0.60$ ). The thickness of an interface element is taken to be zero. The description of the interface element was adopted in ABAQUS program which developed by reference [4]. These elements connect two deforming bodies that slide along each other. Contact load transfer occurs between the nodes of the ISL element, which is attached to one deforming body, and a slide line which is attached to other deforming body. The nodes of the ISL element form the slave surface, and slide along the slide line attached to the master surface. ISL elements have 2 or 3 nodes associated with the "slave" surface. The ordering of the nodes on the slave surface is not important for the calculation of the contact direction. For each node of an ISL element, ABAQUS generates a contact constraint. Hence, the nodes of the ISL element follow the slide line. The Lagrange multiplier method is usual approach for contact constraints in this type of element. The friction forces acting on the contact area follow Coulomb's law. An advantage of this type of interface element is that its constitutive laws are only

dependent on the friction parameter, i.e. it is independent of the bond stress-slip relation. Therefore, this element represents only the chemical adhesion and friction between concrete and steel bar.

### **3.2 Concrete**

As the loading changes from uniaxial to triaxial stress states, a unified approach is advantageous when selecting a constitutive model for concrete. Such a model was proposed recently by Ottosen [5]

In addition, calibration of the model requires only simple data. These data are obtained usually by standard uniaxial tests of the concrete in question. The construction of the model can be conveniently divided into steps:-

- (1)- Failure and cracking criteria.
- (2)- Nonlinearity index
- (3)- Change of the secant value of Young's modulus.
- (4)- Change of the secant value of Poisson's ratio.

In this study, a special smeared crack model is adopted. The constitutive matrix used in this analysis has been derived in detail by reference [6]. Within this model the initiation of a cracking process at any location happens when a principal stress component exceeds a prescribed tensile limit. Upon further loading of singly cracked concrete, a second set of cracks can form in the direction normal to the first set of smeared cracks. Therefore, in that direction, if the concrete stress is less than  $\sigma_t$ , then concrete remains singly cracked. Otherwise, if it is greater than  $\sigma_t$ , then the second set of cracks forms.

## **4- Experimental verification**

To compare numerical results with recent experimental data, the bond stress slip curves of pull-out tests with short embedded length will be used. Numerical results can be compared with experimental results by bond stress slip relation. Lack of detailed experimental results does not permit local bond stress comparison. The additional numerical information on normal stresses and displacements cannot be checked either. The only indication would be the occurrence of splitting cracks in the surrounding concrete.

### **4.1 Data of the test**

The results of a series of tests performed by Malvar [7], comprising 12 pull-out specimens, were used for verifying the pull-out numerical model. In the test series, radial confining pressure around the concrete specimen and radial deformation, together with bond stress and slip, were assumed to be fundamental variables needed to describe the interface behavior property. Only five lugs were in contact with the concrete, contact being prevented in the rest of the specimen by inserting silicon-rubber spacers around the bars. The spacers allowed inclined radial cracks forming at each rib to propagate to the outer concrete surface. The outer concrete surface was surrounded by a threaded steel pipe, which carried the local shear stresses. Most of the steel pipe split longitudinally into

eight strips to prevent any confinement from the pipe itself. An advantage of the split pipe is its two-dimensional confining action, which allows for much higher confinement stresses than reported previously and transfer via shear stresses, which prevents unknown confinements that take place when bearing stresses are present (e.g., as in a standard pullout tests).

Three test series were carried out. The first series were carried out to verify the setup (Tests P0 and P1). For the first and second test series (Test 1 though 5), bars with inclined ribs that formed a 68-deg angle with the longitudinal axis were used. For a # 6 bar, the maximum rib spacing is 13.3 mm (0.525 in). The measured rib spacing was 12.2 mm (0.481 in), and the clear distance between ribs was 9.2 mm (0.36 in). The related rib area was 0.064 in<sup>2</sup>. Of the three series in this investigation only series 2 is considered here. For Tests 1 through 5, the confining pressure was set at 1.5, 4.5, 7.5, 10.5, 13.5 N/mm<sup>2</sup> on the over length of outer surface of the concrete cylinder. In all cases Grad 60, # 6 bars satisfying ASTM A 615-89 were used.

#### 4.2 Geometric modeling and discretization into F.E.

The mesh of the finite elements discretization has already been performed, as shown in Fig. 2. An axis-symmetric non-linear finite element analysis was used to obtain the stresses and deformations in the process zone.

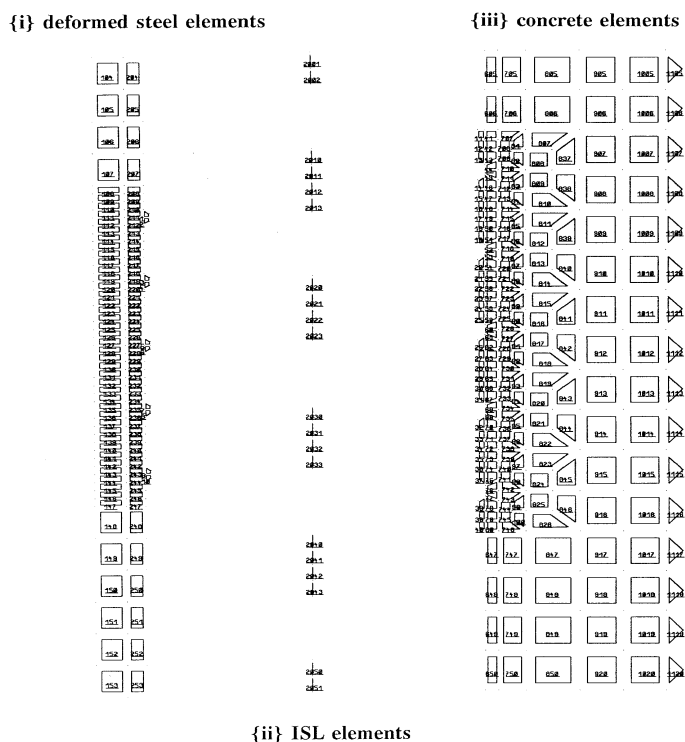


Fig. 2 The mesh of the finite elements

Also, Fig 3 has shown that the mesh was divided into 362 ring elements of various sizes. An advantage of using these interface elements is that its constitutive laws are independent of the bond stress-slip relation. Also, these elements represent only the chemical adhesion and friction between steel and concrete. The friction coefficient of these elements can be, for example, of value 0.3. According to data supplied by Malvar [7], the modulus of elasticity  $E_c$  of the concrete can be taken as  $E_c = 27580 \text{ N/mm}^2$ , Poisson's ratio  $\nu_c = 0.2$ , maximum compressive strength  $\sigma_c = 40.2 \text{ N/mm}^2$ , and maximum tensile strength  $\sigma_t = 5 \text{ N/mm}^2$ . The modulus of elasticity for the steel bar ( $E_s$ ) can be taken  $200000 \text{ N/mm}^2$ , and Poisson's ratio  $\nu_s = 0.3$ .

#### 4- Numerical result

Figures 3 shows the stresses distribution in radial in end longitudinal directions for concrete cylinder. These stresses indicate that the area of the highest compressive stress concentration is in the front of ribs in general. A more severe compressive stress concentration is observed at the rib nearest to the applied load and gradually decreases inwards:

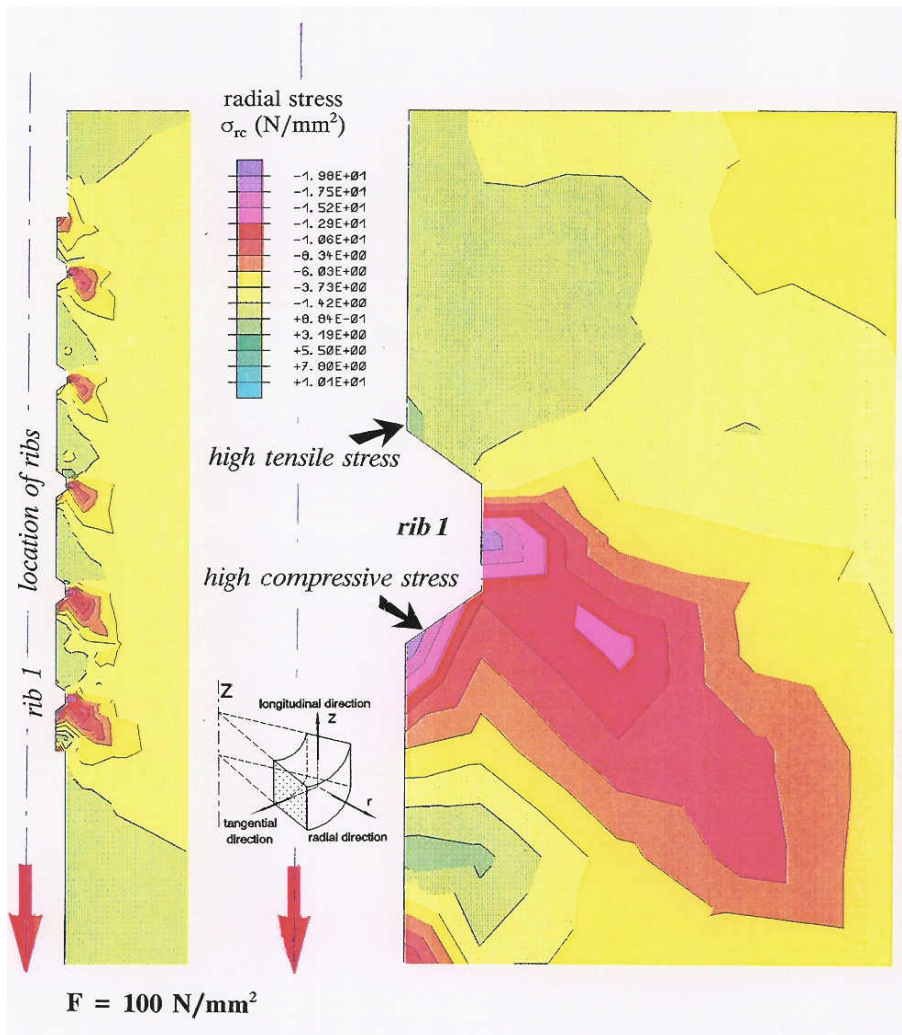


Fig. 3 Radial Stresses

Figure shows the bond stress distribution along the embedded length at different stages of loading. The configuration of bond stress distribution along the embedded length reflects the mechanical behavior of bond between steel and concrete. In the early stage of loading, the bond stress is very small, the main bond strength is transferred in the rib nearest to the applied load and gradually decreases inwards. In this stages, the bond efficiency is assured by chemical adhesion and friction between concrete and steel at the bar surface between ribs.

The increasing of the load gives larger bond stress values in front of ribs while the bond strength reaches a peak and then it starts decreasing behind the ribs, particularly as shown in Fig. 4.

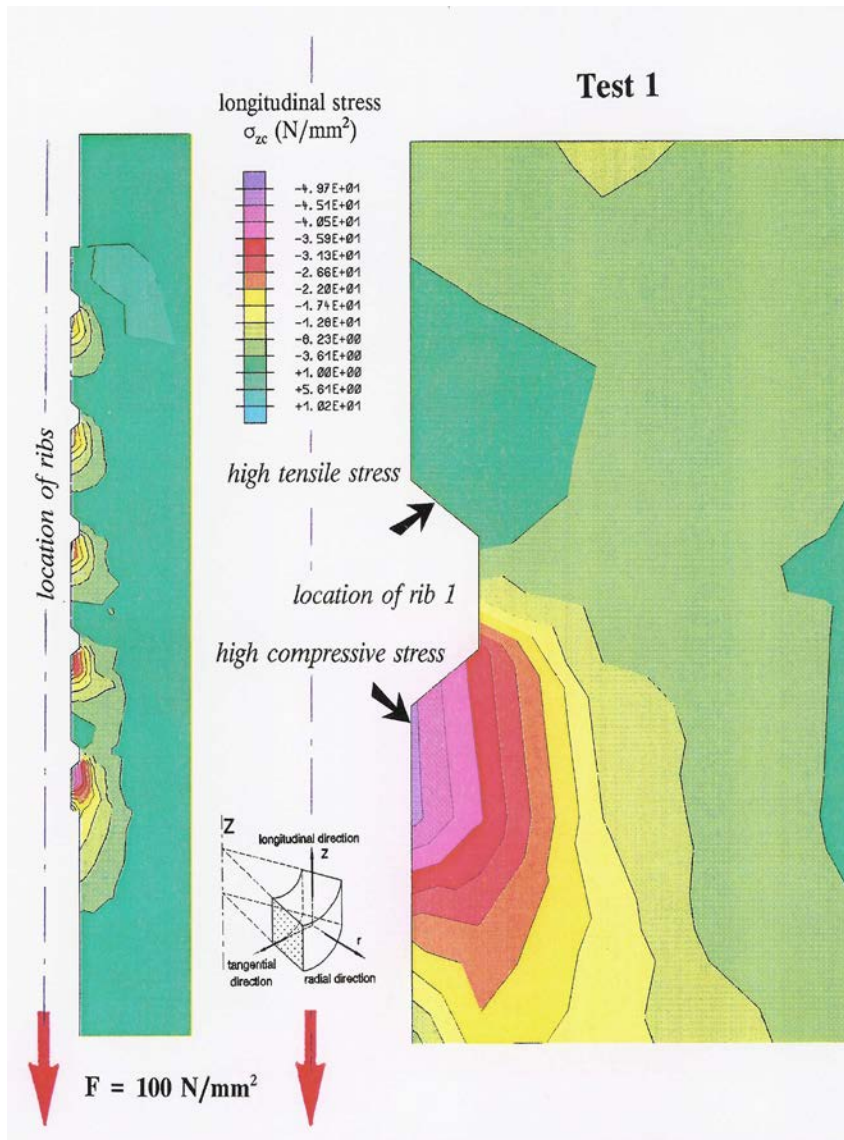


Fig. 4 longitudinal Stresses

It is thought that adhesion between the steel bar and the concrete is lost at these portions. This indicated that chemical adhesion and friction break down between ribs, the ribs of the bar induce large bearing stresses in the concrete, and transverse microcracks originate at the back of ribs. Fig. 5 shows the deformation of a part of cylinder concrete which is adjacent to the steel bar. Figure illustrates that sufficient confining pressure restrains the concrete against splitting and thus increase the ultimate bond stress.

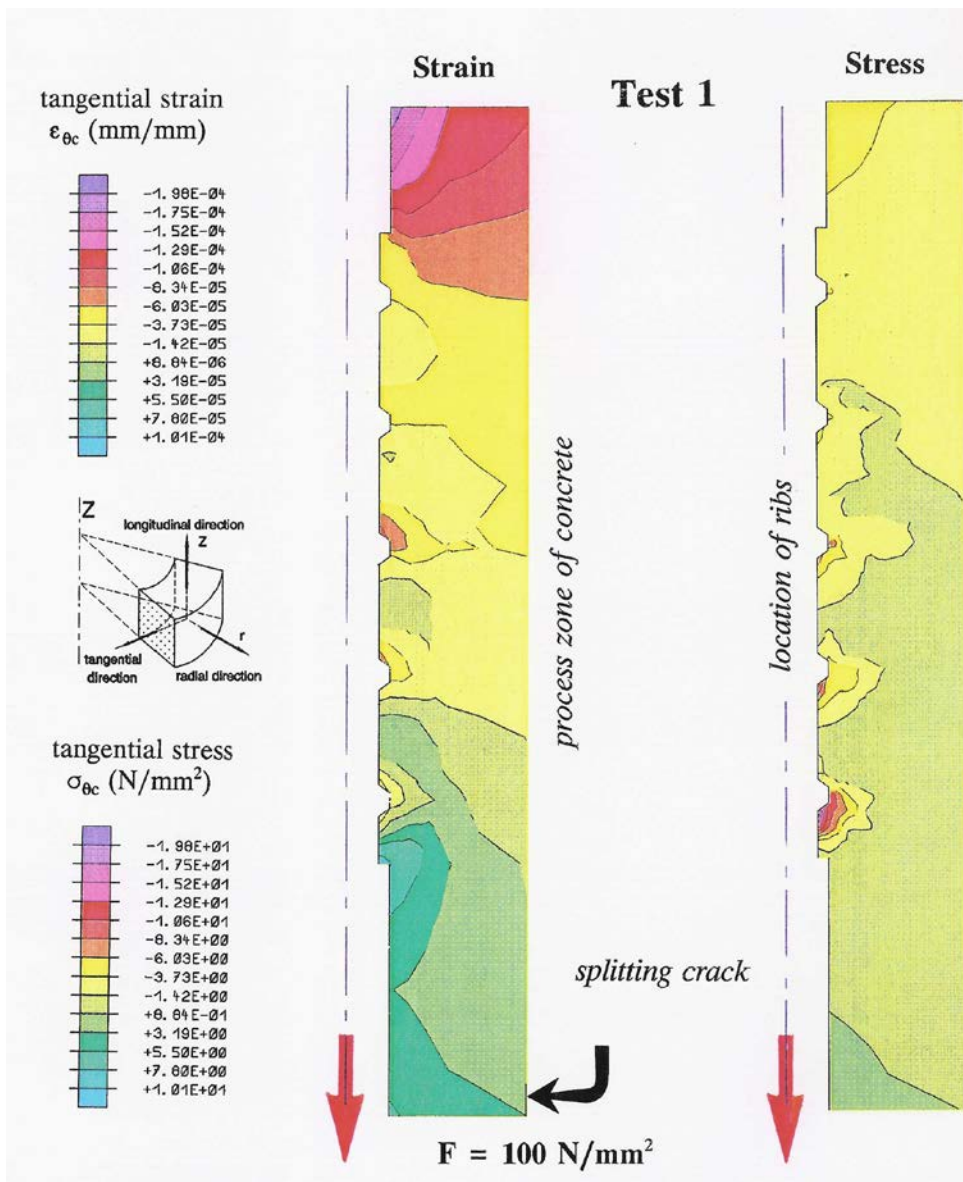


Fig. 5 Tangential Stresses

## 5- Comparison with the experimental results

The further increases in the applied load, the bond stresses in front of ribs increase also. In this stage the bond is assured by bar-to-concrete interlock. Also, it appears that the adhesion has been almost completely broken. Almost at the end of loading, bond behavior tends to become of the dry-friction type, since the concrete keys between the lugs are crushed or sheared off, and the tips of the ribs rub against the concrete. Therefore, the bond between deformed bars and concrete must then depend on the mechanical resistance of ribs and frictional resistance between concrete and steel at the bar surface between ribs shown in Fig 7, Tassios [8], and Goto [9].

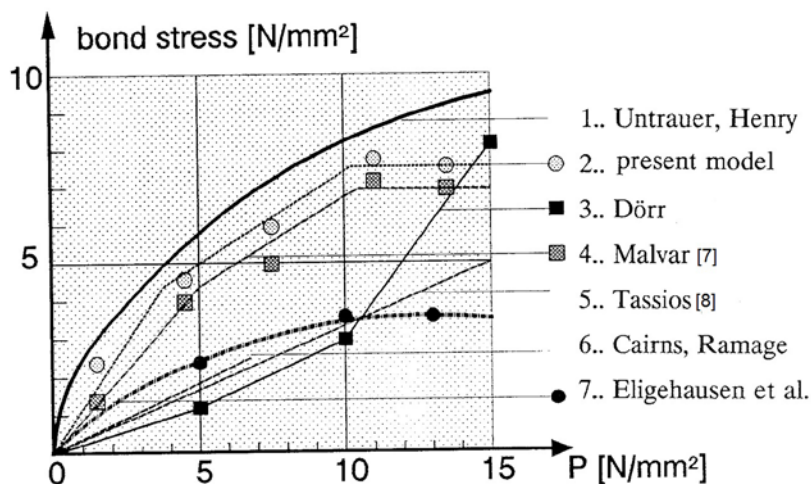


Fig. 7 Different relation between bond stresses and tensile Stresses

Fig. 8 shows the numerical results plotted together with the comparison of experimental results given by Malver [6].

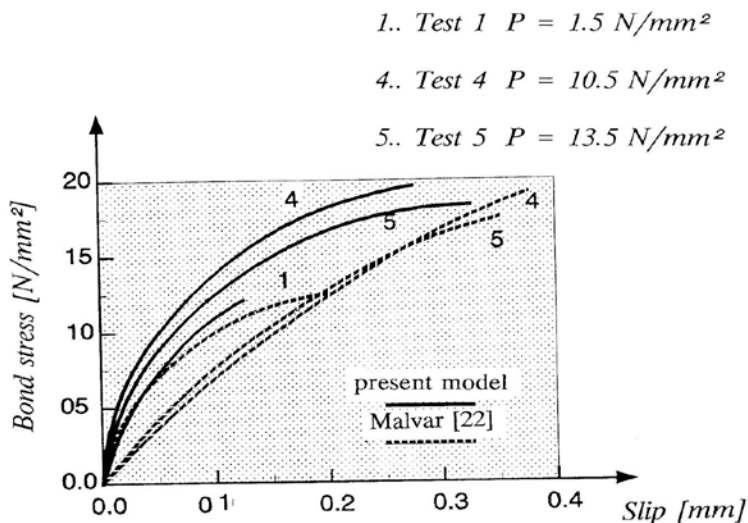


Fig. 8 Comparison numerical with the experimental results

Therefore, the experimental verification was to demonstrate that the bond between deformed reinforcing bars and surrounding concrete can be predicted by numerical analysis taking account of non-linear effects. Thus, it has been concluded that this numerical method is a powerful tool to investigate the bond between steel and concrete. This numerical study contributes to a better understanding of influencing relevant parameters on the basic bond mechanisms and participates in accomplishing experimental research in this area. The curves in this Figure indicate that the numerical analysis is in good agreement with experimental results.

## **References**

- [1] Eibl, J., and Neuroth, U., "Experimentelle und rechnerische Untersuchung zum Einfluß örtlicher Stahldehnungen und Querspannungen auf das local Verbundverhalten von Betonrippenstahl," Forschungsbericht Inst. f. Massivebau der Universität Karlsruhe, Germany, 1989.
- [2] Bennett, E. W., and Snounou, I. G., "Bond-slip Characteristics of plain reinforcing bars under varying stress," Bond in concrete, Edited by P. Bartos, Applied Science Publishers London, 1982, pp. 140-150.
- [3] Gerstle, W., Ingraffea, A. R., and Gergely, P., "the Fracture Mechanics of Bond in Reinforced Concrete," Report 82-7, Dep. Of Struct. Engng. Cornell University, Ithaca, NY, 144pp.
- [4] Hibbitt, Karlsson; and Sorensen, "ABAQUS User's Manual," Software Finite Element Program, V. 1 and V. 2, Version 4.9, 1992.
- [5] Ottosen, N. S., "Constitutive Model for Short-Time Loading of Concrete; ASCE Journal of the Engineering Mechanics, V. 105, No. EM1, 1979, pp.127-141.
- [6] Schlüter, F. H., "Dicke Stahlbetonplatten unter stoßartiger Belastung (Flugzeugabsturz)," Massivbau und Baustofftechnologie Karlsruhe, Heft 2, Germany, 1987.
- [7] Malvar, L. Javier, "Bond of Reinforcement Under Controlled Confinement," ACI Material Journal, V. 89, No. 6, Nov.-Dec. 1992, pp. 593-601.
- [8] Tassios, T. P., "Properties of Bond Between Concrete and steel under Cycles Idealizing Seismic Actions," in Proceedings of AICAP-CEB Symposium, Rome, Apr. 1979, CEB Bulletin No. 131, Paris, pp. 67-122.
- [9] Goto, Y., "Crack Formed in concrete Around Deformed Tension Bars," Journal of the ACI, 1971. pp. 244-251.